DOI: 10.6060/mhc245851k

Optical Properties of Complexes Based on Metal Phthalocyanines and Oxygen-Free Graphene

Inna V. Klimenko,[a@] Elena A. Trusova,[b] and Anton V. Lobanov[a,c]

[a]*N.M. Emanuel Institute of Biochemical Physics, Russian Academy of Sciences, 119334 Moscow, Russia*
[b]*A.A. Baykov Institute of Metallurgy and Materials Science, Russian Academy of Sciences, 119334 Moscow, Russia*
[c]*Moscow Pedagogical State University, 119991 Moscow, Russia*
[@]*Corresponding author E-mail: inna@deom.chph.ras.ru*

Dedicated to the memory of Academician of Russian Academy of Sciences Oskar I. Koifman

Two hybrid systems based on oxygen-free graphene and AlCl- and Zn-phthalocyanines have been synthesized in aqueous-organic medium and comparatively studied by optical absorption method. N,N-Dimethylformamide was used as an organic solvent. It has been shown that the presence of oxygen-free graphene in the systems prevents the aggregation of phthalocyanines in aqua medium and contributes to their stabilization in monomeric form. The stability of the resulting hybrid complexes as well as the binding capacity of the components of the systems has been evaluated. The mechanisms of phthalocyanines and oxygen-free graphene interaction in aqueous-organic medium have been proposed.

Keywords: Zinc phthalocyanine, aluminum phthalocyanine chloride, oxygen-free graphene, hybrid structures, aggregation, optical absorption.

Оптические свойства комплексов на основе металлфталоцианинов и бескислородного графена

И. В. Клименко,[a@] Е. А. Трусова,[b] А. В. Лобанов[a,c]

[a]*Федеральное государственное бюджетное учреждение науки «Институт биохимической физики им. Н.М. Эмануэля» Российской академии наук, 119334 Москва, Россия*
[b]*Федеральное государственное бюджетное учреждение науки «Институт металлургии и материаловедения им. А.А. Байкова» Российской академии наук, 119334 Москва, Россия*
[c]*Федеральное государственное бюджетное образовательное учреждение высшего образования «Московский педагогический государственный университет», 119991 Москва, Россия*
[@]*E-mail: inna@deom.chph.ras.ru*

Две гибридные системы на основе бескислородного графена и AlCl- и Zn-фталоцианинов были синтезированы в водно-органической среде и изучены методом оптического поглощения. N,N-Диметилформамид использовали в качестве органического растворителя. Было показано, что присутствие в системах бескислородного графена препятствует агрегации фталоцианинов в водной среде и способствует их стабилизации в мономерной форме. Были оценены стабильность полученных гибридных комплексов, а также связывающая способность компонентов систем. Предложены механизмы взаимодействия фталоцианинов и бескислородного графена в водно-органической среде.

Ключевые слова: Фталоцианинат цинка, фталоцианинат алюминия, бескислородный графен, гибридные структуры, агрегация, оптическое поглощение.

Introduction

The study of photobiological processes, including the electron and energy transfer, absorption of a quantum of light by a biological molecule, intramolecular energy redistribution, formation of a primary photoproduct, fluorescence and bioluminescence, is the most important research problem of modern biophysics. Most biological objects have photosensitivity as a result of absorbing light quanta by molecules of chromophores, proteins, pigments and nucleic acids.

Tetrapyrrole compounds (TCs), which include chlorins, porphyrins, phthalocyanines and their metal complexes, take special place among compounds capable of photosensitizing biological tissues. They are successfully used in photodynamic therapy (PDT) and diagnostics of cancer tumors as photosensitizers (Ps) (photoactive natural or synthesized compounds).[1-9]

The presence of Ps is a key factor in PDT; which mechanism of action is based on the ability of Ps to accumulate selectively in target tissues and when irradiated with light at a wavelength corresponding to the maximum absorption of Ps generate singlet oxygen $^1O_2$ and other reactive oxygen species (ROS) such as $O_2^{-\bullet}$, $HO^\bullet$ and H_2O_2. $^1O_2$ and other ROS play a key role in the photodynamic process.[10-13] The interaction of $^1O_2$ and cytotoxic oxygen species with biological objects leads to oxidative damage and destruction of vital organelles of targeted cells and, therefore, to necrosis, apoptosis or autophagy of the target tissue.

For the productive action of TCs and their metal complexes in various biomedical applications, including PDT, it is necessary to solubilize tetrapyrroles in aqueous media and, secondly, the presence of TCs molecules in the system in a monomeric form, which allows in the absence of annihilation processes of triplet excited states to launch the triplet-triplet energy transfer mechanism to oxygen, also is required. However, upon contact with aqua and aqueous physiological solutions, TCs have a stable tendency to aggregate with the formation of dimers and other types of aggregates, which reduce the photodynamic activity of TCs.[14,15]

Aggregation of TCs is a well-known phenomenon and is widely discussed in the literature.[8,13-20] The photophysical properties of TCs strongly depend on the monomer/aggregate ratio in the system; in particular, the presence of dimers, trimers and other aggregated species of TCs lead to a significant shift of the absorption bands compared to the absorption characteristics of the monomeric TCs. The presence of aggregates can lead to fluorescence quenching, which is usually significant for TCs monomers. On the other hand, in diagnostics it is important to use TCs that do not cause phototoxic side effects, which can be achieved through the targeted formation of the certain type aggregates with additional solubilizers and auxiliary macromolecular carriers. The study of the TCs aggregation behavior, which also includes the using of optical methods, is important both for understanding the fundamental physicochemical properties of TCs, and when developing the possible ways of industrial application, including the biomedical applications as Ps.

It is known, that phthalocyanines (Pcs) obtained by Brown and Cherniyak[21] in 1907, as well as Pc metal complexes, are promising Ps. Pcs are structural derivatives of porphyrins and, due to their outstanding photophysical and photochemical properties, stability, structural versatility, the presence of semiconductor and magnetic properties, are the objects of numerous studies. Pcs are widely used as active components of various supramolecular systems, supramolecular ensembles and nanomaterials.[22]

All Pcs (known systematically as tetraazatetrabenzoporphyrins) are intensely colored two-dimensional macroheterocyclic compounds having four isoindole groups, linked by four nitrogen atoms. Pc have five conjugating contours and a special electronic delocalization of the 18-π aromatic system, reinforced by condensed benzene rings, which causes a deep Pc color and is related to the porphyrins. They have good absorption in the UV-Vis region (in the B-band at ~300–400 nm and the Q-band at ~600–700 nm, (the so-called "therapeutic window")), a long triplet life time (0.1–1 ms) and a high quantum output of singlet oxygen (Φ_Δ=0.91).[20,23-30] Pcs, being chromophores and like others TCs, have an efficient complexation ability relative to different metals.[8] At least 70 elements of the periodic table are capable of being in the place of centrally coordinated atoms[15,31] and to integrate with Pc in the central cavity to form phthalocyanine metal complexes (MePc).[15] As a result, the geometries as well as the electronic and other desirable properties of Pc can be improved.[15]

Several methods for inhibiting Pc aggregation in biochemical systems and liquid media are known. They include the modification of the macrocycle by replacing hydrogen atoms with various groups, such as alkyl, aryl, aryloxy, alkoxy, phenoxy and others, the introduction of bulk substituents that create steric difficulties for contact between macrocycles, including sulfonyl, carboxylic acid and amino group, a replacement of the complex-forming metal in the Pc molecule, the synthesis of one-dimensional nanowire crystals of MePc, the synthesis of phthalogen conjugates with carbohydrates and formation of related MePc complexes with carbohydrates, the use of vector drug delivery systems, the use of liposome medium, serum proteins, magnetic emulsion with nanostructured colloidal particles and biocompatible polymer nanoparticles, *etc*.[22, 32-41]

Also, one way to solve this problem and to stabilize the monomeric forms of MePc in the biological media and aqueous solutions is to create various supramolecular systems or supramolecular ensembles with effective intermolecular interactions. In our previous works, we proposed the use of various biocompatible water-soluble excipients in complex with chlorin e_6 (Xe_6) to reduce the hydrophobicity of TPs and their aggregation in aqueous solutions.[5,42,43] In addition, a method that makes it possible to prevent the aggregation of TPs is their immobilization on the surface of an inert solid support, which inhibits aggregation of Pc macrocycles. In this case, the complex formation with the participation of theranostic two-dimensional (2D) nanomaterials, for example, graphene or materials based on it, as part of a hybrid system, and phthalocyanine complex takes place.[44] This graphene-Pc hybrid supramolecular structure will be useful in binding photo- and/or redox chromophores to graphene through self-assembly, as well as charge transfer in complexes.

Developing this direction, in the presented work we synthesized and comparatively studied by optical absorp-

tion method two hybrid systems based on oxygen-free graphene (OFG) and AlCl- or Zn-phthalocyanines (AlClPc and ZnPc). Oxygen-free (non-oxidized) graphene was chosen because, of the many varieties of graphene, only in it all the carbon atoms have sp^2-hybridized orbitals, combined into a π-system with a high potential for coordination interaction. Only it contains a minimal amount of oxygen-containing groups located along the periphery of the sheets. An oxygen-free graphene suspension was obtained by a sonochemical method in an acidified with nitric acid mixture of N,N-dimethylformamide (DMF)–aqua at a DMF concentration of 4.7 vol.%.

Both phthalocyanines are promising second-generation photosensitizers and demonstrate the combination of physical, chemical and biological properties necessary for PDT.[15,30,44-52] The choice of the polar aprotic solvent DMF is explained by its high solvation ability and donor-acceptor properties. DMF interacts with the central metal atom in MePc molecule through the terminal oxygen atom. Moreover, DMF is a solvent which is often used in small quantities in pharmaceutical and biomedical fields due to its high dissolving power.[15]

Experimental

A metal phthalocyanine complexes stock solutions (AlClPc, chloro(29H,31H-phthalocyaninato)aluminium, with chloride extraligand and ZnPc, zinc tetrabenzo[5,10,15,20]tetraazaporphyrin, both obtained from Acros Organics, Belgium,) with the concentrations of $1.18 \cdot 10^{-3}$ mol/L and $1.32 \cdot 10^{-3}$ mol/L, respectively, were prepared by dissolution of MePc dry samples (0.0152 g) in 20 mL of N,N-dimethylformamide (DMF, Reakhim, Russia). The resulting concentrations were specified from electronic absorption spectra. The purity of crystalline MePc was confirmed with MALDI mass spectrometry on a Thermo DSQ II device (United States). The stock solutions were stored in the dark at 4 °C and, if necessary, were diluted before the experiment (0.02 mL of the stock solution of metal phthalocyanine complexes of AlClPc or ZnPc per 8 mL of DMF, hereinafter called a base solution).

A suspension of oxygen-free graphene (OFG) was obtained by ultrasonic irradiation of graphite powder in a DMF/aqua mixture at a volume ratio of 1/30, for which a Sonoswiss SW1H brand unit with a power of 200 W (Switzerland) was used. Synthetic graphite powder with particle sizes 500–750 mm (Unikhimtek, Russia) was used as the initial carbon species, its purity was 99.99% and impurities presented were of sulfur and chloride ions (less than 10 ppm). An acidified mixture of DMF (Reakhim, Russia) and deionized aqua were used as a dispersion medium to stabilize the graphene suspension. Deionized aqua was produced in a reverse osmosis Raifil system. A batch of graphite powder (0.5 g) was mixed with 30 mL of DMF solution in water, and then p*H* value of the medium was brought to the value 3 by adding HNO_3. The exfoliation process was carried out at 60°C for 30 min. The resulting graphene suspension was separated from unreacted graphite by decanting and allowed to stand for 20–24 h, after which it was re-decanted. Light and medium graphene suspension fractions were used in the subsequent syntheses of hybrid nanostructures.

The hybrid systems MePc-OFG in aqueous-organic media were synthesized in a K10 standard quartz cuvette with a path length of 1 cm for immediate spectrophotometric studies of systems with different graphene concentrations. 2 mL of MePc base solution was placed into the cuvette and then titrated with a suspension of graphene in an aqueous solution of DMF using a 0.1 mL aliquot; a total of 0.1–1.0 mL of the suspension was consumed for one titration. The MePc reference solution was prepared by adding 0.02 mL of the MePc - DMF stock solution to 8 mL of the DMF-water mixture so, that the DMF concentration in the final solution was 4.7 vol%. All solvents in our experiments were of analytical grade and were used without further purification. All spectrophotometric data obtained after adding graphene suspensions were normalized to the initial volume (V_1=2 mL) of MePc-DMF solutions according to the formula: $D=D_0/K$, where $K = (V_1 + V_{gr})/V_1$. In this formula, D and D_0 are the normalized and experimental values of the optical density of the solution, respectively, V_1=2 mL is the initial volume of MePc-DMF solution, V_{gr} is the volume of the graphene-DMF-H_2O suspension used for titration (0.1–1.0 mL).

The presence of AlClPc and ZnPc aggregates, the degree of their impact on the optical absorption spectra of the initial solutions, the role of graphene in the MePc aggregation process were determined using a UV-1900 spectrophotometer (Beijing Purkinje General Instr. Co. Ltd.). The morphology of the obtained graphene suspensions and electron diffraction on its sheets were investigated with TEM by using the LEO-912 AB OMEGA instrument (LEO Carl Zeiss, operating at 100 kV. EELS data were obtained on the JEM 2010 instrument (JEOL Ltd.) equipped with energy dispersive spectrometry (EDS; Inca, Oxford Instruments) and electron energy loss spectrometry (EELS; GIF Quantum, Gatan Inc.) attachments; accelerating voltage was 160 kV. The thickness and the number of layers in the flakes were calculated based on 5–10 measurements on each of 5–6 TEM mages for each graphene suspension sample.

Results and Discussion

It is known that all spectral properties of Pcs are connected qualitatively with the presence of four frontier orbitals: the HOMO, HOMO-1, LUMO, LUMO+1.[15,53,54] There are two principle types of $\pi \rightarrow \pi^*$ transitions from the highest first occupied molecular orbital (HOMO, HOMO-1) to the lowest unoccupied molecular orbitals (LUMO, LUMO+1) of the metal complex. Both Q and B (Soret) bands arise from $\pi \rightarrow \pi^*$ transitions and according to Gouterman's model[53] are explained in terms of a linear combination of transitions from a_{1u} and a_{2u} HOMO orbitals to the doubly degenerate e_g LUMO orbitals.

In the absorption spectra of AlClPc and ZnPc in DMF solutions (Figure 1, curves 1 and 3, respectively) we can observe $\pi \rightarrow \pi^*$ transitions from the highest occupied molecular orbital (HOMO) to the lowest unoccupied molecular orbital (LUMO) of the metal complex which represent Pc absorption bands. First type: the B-band located at 300–450 nm, which is a characteristic of all MePc, with the absorption maxima of ~349 nm for AlClPc and ~339 nm for ZnPc, equivalented to the Soret band (Y-band) in porphyrins and attributed to the $a_{2u}(\pi) \rightarrow e_g(\pi^*)$ together with $b_{2u}(\pi) \rightarrow e_g(\pi^*)$ transitions and the lowest allowed $n \rightarrow \pi^*$ transition. Second one: the stronger Q band, located at 600–700 nm with an absorption maxima at λ_{QI} = 672 nm for AlClPc and λ_{QI} = 669 nm for ZnPc and their vibrational satellites of low intensity at λ_{QIII} = 607 nm for AlClPc and λ_{QIII} = 603 nm for ZnPc, accordingly, which are attributed to the monomeric form of the dye. The shoulder in the region of λ_{QII} at ~ 640 nm is generally referred to H-aggregates of Pc in the DMF solution which due to dimerization/aggregation of the Pc.[55,56] However, based on our theoretical calculations of the absorption spectra of AlClPc in DMF solution[15] we attribute this shoulder to vibronic transitions at ~640 nm (Q_{II}). The absence of absorption in the 710–850 nm absorption region (Figure 1, curves 1 and 3) indicates the absence

of AlClPc and ZnPc J-aggregates with a strictly ordered structure in DMF. Q band is responsible for the color of the compound and is equivalented to the α band in porphyrins and attributed to the $a_{1u}(\pi) \rightarrow (\pi^*)$ transition. Q band splitting into two bands Q_I and Q_{II} can be also observed due to exciton coupling between two nonequivalent molecules in a unit cell (Davydov splitting[57,58]).

Also, the AlClPc-DMF-aqua and the ZnPc-DMF-aqua systems were examined for the lines shape change and the shifts of the Soret and Q-bands (Figure 1, curves 2 and 4). As expected, a significant broadening of the spectrum lines, a sharp decrease in the intensity and the broadening of the Q-bands, as well as the shifts of the absorption spectrum maxima to the short-wave region are observed for the AlClPc-DMF-aqua and ZnPc-DMF-aqua systems. These changes in the absorption spectrum are due to the aggregation behavior of MePc, namely, a sharp decrease in the content of AlClPc and ZnPc monomers in the DMF-aqua mixtures and a significant increase in the content of H-aggregates and rarely observed J-aggregates of MePc.

The presence of graphene in the initial suspension was confirmed by the following methods: transmission electron microscopy (TEM), dynamic light scattering spectroscopy (DLS), IR spectroscopy and Raman spectroscopy.[59] It was found that a DMF/aqua mixture stabilizes a suspension of oxygen-free graphene for several weeks, therefore, it can be used to protect pigments from photo degradation in aqua. Graphene-containing hybrid complexes we prepared by titration of 2 mL of MePc solutions in DMF with a suspension of graphene in DMF-aqua mixture (0-2 mL). Figure 2*a* shows a TEM image of 3D graphene particles, typical of the suspension used in a DMF-aqua mixture, whose dimensions about 400–500 nm. The electron diffraction pattern, which is a combination of reflections of almost equal intensity, also indicates the predominance of multilayer graphene particles in the suspension (Figure 2*b*). As we have shown previously, ultrasonic exfoliation in DMF/aqua mixture leads to the production of a suspension of oxygen-free graphene with a trimodal size distribution: 475(±82) nm – 62%, 918(±108) nm – 20% and 2630(±878) nm – 18%.[59] According to EELS analysis, graphene oxide was absent in the obtained graphene: 532 eV peak corresponding to oxygen does not appear in the spectrum (Figure 3*c*). At the same time, peak at the region of 284–289 eV corresponds to 1s → π∗ transition and shows the presence of pure oxygen-free graphene, the sheets of which form associates of different layers, denoting the presence of C_{sp2}.[60]

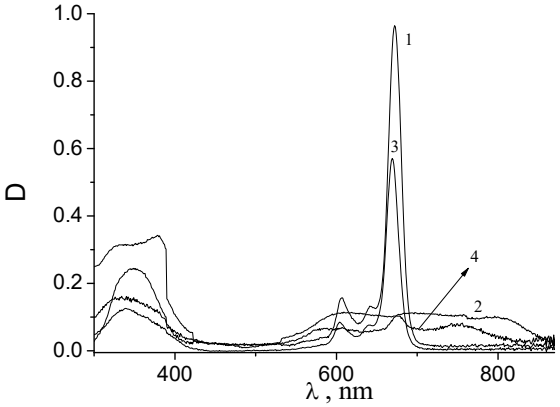

Figure 1. UV-Vis spectra of AlClPc in DMF (C_{AlClPc}= 2.99·10^{-6} mol/L) (1) and DMF-aqua mixture (C_{H20}=15 vol. %) (2) and ZnPc in DMF (C_{ZnPc} = 3.3·10^{-6} mol/L) (3) and DMF-aqua mixture (C_{H20}=15 vol. %) (4).

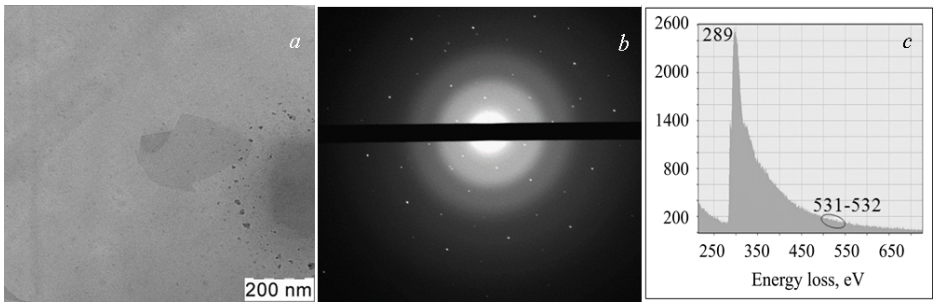

Figure 2. TEM image of graphene particles in DMF-aqua mixture (*a*), electron diffraction on them (*b*) and EELS analysis of graphene suspension (*c*).

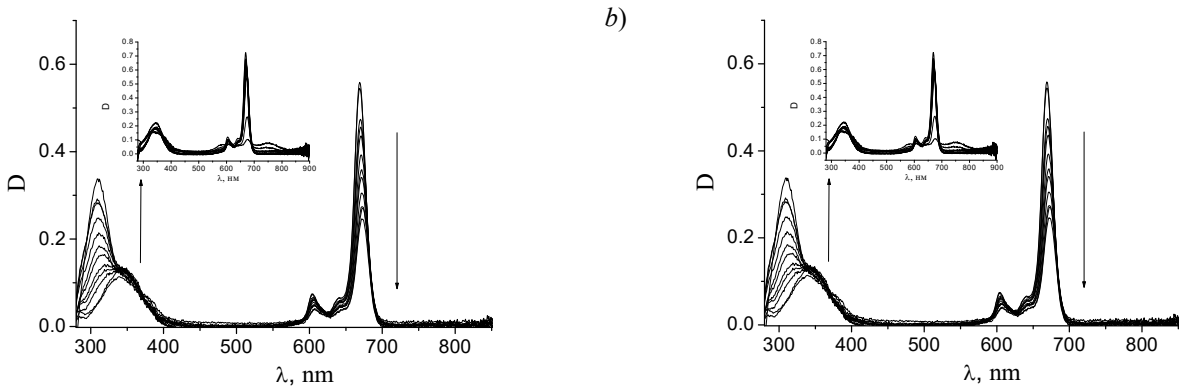

Figure 3. UV-Vis spectra of AlClPc-graphene-DMF-aqua (*a*) and ZnPc-graphene-DMF-aqua (b) hybrid systems obtained by adding 0.1 – 1 mL of graphene suspension in DMF-aqua mixture to 2 mL of MePc-DMF solution. Arrows show an increase in the concentration of graphene suspension in the systems. Insets show spectra for the systems obtained when titrating MePc solutions with DMF-aqua solution.

Figure 3 shows how the optical absorption spectra of AlClPc and ZnPc change during the titration of their solutions with a 0.1 mL aliquot of a graphene suspension in a DMF/aqua mixture. Their analysis shows that the interaction of MePc with OFG leads to significant changes in the electron absorption spectra of AlClPc and ZnPc. In contrast to the typical changes in spectra of MePc in the presence of aqua (the increase in scattering intensity, connected with the increase in aggregates size, insets in Figure 3), the intense absorption is observed in the regions of ~230–400 nm with maxima at ~305 nm (Figure 3*a*) and ~309 nm (Figure 3b). They are the combination of the B-band (Soret) of the electron absorption spectra of monophthalocyanines and $\pi \rightarrow \pi^*$ transitions in graphene.[28] A shift of the B-band maximum towards long wavelengths as the graphene concentration in the both systems increases and appearance of the isobestic point of both spectra (Figure 3*a*,*b*), when adding the first doses of graphene suspension, are probably the criteria of the charge transfer complexes formation. Moreover, the appearance of an isobestic point on both spectra indicates the stability of adducts (direct attachment products), namely, the Pc-graphene complexes obtained without the formation of intermediates.

In the Q-band region (Figure 3*a*,*b*), a hypsochromic effect is observed and there are no absorption maxima in the region of 705–780 nm, which differs from the data given in the insets in Figures 3*a*,*b* and 1 (curves 2,4). This is due to the sequential decrease in the concentration of unbound MePc and the sequential disaggregation of MePc upon the addition of graphene. As for systems without graphene (Figure 3, insets), it should be noted that the differences in the shape of the AlClPc-aqua-DMF spectrum bands compared to the ZnPc-aqua-DMF ones are connected with the loss of symmetry in AlClPc molecule. This occurs due to the distortion of the dye molecule in the presence of aqua because of the coordination interaction of the aluminum atoms and the oxygen ones in the aqua molecules.[15] This axial coordination of AlClPc probably provides a strong bond between the phthalocyanine metal complex and its environment (solvent molecules). Also, the shift of the metal ion from the macrocyclic plane in the presence of graphene in the system, caused by interaction between the metal ion and the π-system of graphene, results to the dissociation of the dimers of the MePc complexes, just as it was described by the authors of the work,[61] devoted to the study of electronic and steric effects affecting the self-assembly of porphyrazine in the presence of the π-system of the ligand.

The observed shifts of the short-wavelength shoulders λ_{QII} at ~640 nm to the long-wavelength region, corresponding to the $S_{0.0} \rightarrow S_{1.1}$ transitions, and the decrease in their intensities (Figure 3) also indicate an increase in the distance between molecules in H-aggregates, formed earlier in the presence of water. Apparently, this is because when titrated with a graphene suspension, its sheets cause the separation of MePc H-aggregates.

It should be noted that the binding capacity of different types of carbon varies significantly. A striking feature of the discussed supramolecular hybrid complexes is their high stability, due to the strong coordination interaction of its constituent parts, apparently due to the high coordination ability of sp^2-hybridized electron orbitals of the graphene carbon atoms of OFG, which distinguishes it from other types of nanocarbon. In our case, to evaluate the stability of the obtained complexes the binding constant K_b using the Benesi-Hildebrand ratio[62-65] was determined from the absorption spectra (Figure 3). The equation $\lg((D_i–D_0)/(D_f–D_0)) = \lg(C) + \lg(K_b)$ was used, where D_0, D_i and D_f are the absorption values for the initial (in the absence of graphene), intermediate and final point at the absorption wavelength corresponding to the monomeric form of the dye, C is the concentration of the added component, that is, the graphene suspension.

Taking into account the DLS data confirming the multilayer nature of the resulting graphene, three-layer graphene with a trimodal size distribution was adopted as a model structure, as mentioned above.[59] The binding constant (K_b) was determined by straightening the titration curve in linearizing coordinates, where $y = \lg((D_i–D_0)/(D_f–D_0))$ and $x = \lg(C_{gr})$.

Considering the optical absorption data obtained for AlClPc-graphene-DMF-aqua systems, the equation of the lines $y = 0.4752x + 3.26$, $y = 0.4758x + 3.4$ and $y = 0.4736x + 3.61$ with the corrected coefficients of determination $R^2_{adj} = 0.9915 \div 0.9926$, as well as the values of the segment clipped on the x-axis, $K_b=(1.8\div4)\cdot10^3$ L/mol were calculated for each fraction of graphene particles. The obtained values indicate, that different binding mechanisms are realized in the synthesized charge transfer complexes. At present, the impact of the solvent on the mechanism of graphene-Pc interaction has been poorly studied, but it certainly must be taken into account in calculations of a realistic model. We have previously shown that the stabilization of graphene particles in an acidified organic-aqua suspension is ensured by their van der Waals interaction with the cyclic complex $DMF\cdot H_2O$ protonated at the nitrogen atom.[59] Also, in our previous work, we proposed a mechanism for the interaction of AlClPc molecules and graphene particles stabilized by this complex due to the Coulomb interaction sp^2-hybridized electron orbitals of the graphene carbon atoms.[28]

For ZnPc-graphene hybrid complexes in aqueous-organic media, we obtained the following calculated values: $R^2_{adj} = 0.9813 \div 0.9896$, the equation of the lines $y = 1.46689x+10.1594$, $y = 1.4682x+10.6105$ and $y = 1.4667x+11.3019$ for each fraction of graphene particles of certain sizes (475±82 nm (62%), 918±108 nm (18%) and 2630±878 nm (20%), respectively) and the binding constant $K_b=(1.4\div20)\cdot10^{10}$ L/mol. These high values of K_b indicate a strong binding of ZnPc with the graphene particles in a binary DMF-aqua solution. The formation of the complex occurs during the direct interaction of ZnPc and the graphene sheets without the formation of intermediates.

Conclusions

Two hybrid complexes based on metal (Al, Zn) phthalocyanines and OFG were characterized as the possible photosensitizers for PDT. They show intense absorption in the region of characteristic monomeric species with a slight shift to longer wavelengths. The obtained estimated values of the binding constants of the complexes (K_b) confirm our previously proposed mechanism for the

formation of complex hybrid systems based on OFG and MePc complexes. Thus, the photo-chemical investigations confirm promise in further studies of MePc-graphene hybrid complexes. This opens new prospects for the application of such systems for drug delivery and diagnosis.

Acknowledgements. The work was carried out within the state assignments of IBCP RAS (theme No. 122041400110-4) and according to government assignments No. 075-00320-24-00 (IMET RAS).

References

1. Plekhova N., Shevchenko O., Korshunova O. *et al. Bioengineering (Basel*) **2022**; *9*, 82. doi: 10.3390/bioengineering9020082.
2. Abrahamse H., Hamblin M.R. *Biochem. J.* **2016**, *473*, 347–364. doi:10.1042/BJ20150942.
3. Nyman E.S., Hynninen P.H. *J. Photochem. Photobiol. B: Biology* **2004**, *73*, 1-28. doi:10.1016/j.jphotobiol.2003.10.002.
4. Rosenthal I. *Photochem. Photobiol*. **1991**, *53*, 859–870. doi: 10.1111/j.1751-1097.1991.tb09900.x.
5. Klimenko I.V., Lobanov A.V. *J. Biomed. Photon. Eng*. **2016**, *2*, 040310. doi: 10.18287/JBPE16.02.040310.
6. Bonneau S., Vever-Bizet C. *Expert Opin. Ther. Patents* **2008**, *18*, 1–15. doi: 10.1517/13543776.18.9.1011.
7. Martinez De Pinillos Bayona A., Mroz P., Thunshelle C., Hamblin M.R. *Chem. Biol. Drug Des*. **2017**, *89*, 192–206. doi: 10.1111/cbdd.12792.
8. Basova T.V., Belykh D.V., Vashurin A.S. *et al. J. Structural Chem*. **2023**, *64*, 766-852. doi:10.1134/S0022476623050037.
9. Koifman O.I., Ageeva T.A., Beletskaya I.P. *et al. Macroheterocycles* **2020**, *13*, 311–456. doi: 10.6060/mhc200814k.
10. Staicu A., Pasc A., Nuta A., *et al. Rom. Rep. Phys.* **2013**, *65*, 1032–1051.
11. Bonnett R. *Chemical Aspects of Photodynamic Therapy*. Gordon and Breach Science, Canada, **2000**. 324 p.
12. Madkour L.H. The Roles and Mechanisms of ROS, Oxidative Stress, and Oxidative Damage In: *Retracted Book. Nanoparticles Induce Oxidative and Endoplasmic Reticulum Stresses. Nanomedicine and Nanotoxicology* (Madkour L.H., Ed.), Springer, Cham., **2020**, p. 139–192. doi: 10.1007/978-3-030-37297-2_4.
13. Berezin D.B., Makarov V.V., Znoyko S.A. *et al. Mendeleev Commun*. **2020**, *30*, 621–623. doi: 10.1016/j.mencom.2020.09.023.
14. Zhang J., Jiang C., Longo J.P.F. *et al. Acta Pharm. Sin. B* **2018**, *8*, 137–146. doi: 10.1016/j.apsb.2017.09.003.
15. Klimenko I.V., Astakhova T.Yu., Timokhina E.N., Lobanov A.V. *J. Biomed. Photon. Eng.* **2023**, *9*, 030301-1. doi: 10.18287/JBPE23.09.030301-1.
16. Ohno O., Kaizu Y., Kobayashi H. *J. Chem. Phys.* **1993**, 99, 4128–4139. doi: 10.1063/1.466109.
17. Gradova M.A., Gradov O.V., Lobanov A.V., *et al. J. Porphyrins Phthalocyanines* **2022**, *26*, 708–718. doi: 10.1142/S108842462 2500626.
18. Jayme C.C., Calori I.R., Cunha E.M.F., Tedesco A.C. *Spectrochim. Acta A* **2018**, *201*, 242–248. doi: 10.1016/j.saa.2018.05.009.
19. Lebedeva N.S., Petrova O.V., Vyugin A.I. *et al. Thermochim. Acta* **2004**, *417*, 127–132. doi: 10.1016/j.tca.2004.01.023.
20. Tsubone T.M., Braga G., Vilsinski B.H., *et al. J. Braz. Chem. Soc.* **2014**, *25*, 890–897. doi: 10.5935/0103-5053.2014005821.
21. Braun A., Tcherniac J. *Ber. Dtsch. Chem. Ges.* **1907**, *40*, 2709. doi: 10.1002/cber.190704002202
22. Zvyagina A.I. *Colloid J.* **2022**, *84*, 633–641. doi: 10.1134/S1061933X22700090.
23. Ali H.E.A., Piskin M., Altun S., *et al. J. Lumin.* **2016**, *173*, 113–119. doi: 10.1016/j.jlumin.2015.12.010.
24. de la Torre G., Nicolau M., Torres T. Phthalocyanines: Synthesis, Supramolecular Organization, and Physical Properties. In: *Supramolecular Photosensitive and Electroactive Materials*; Elsevier: Amsterdam, Netherlands, **2001**. p. 1–111.
25. Claessens C. G., Hahn U., Torres T. *Chem. Rec.* **2008**, *8*, 75–97. doi: 10.1002/tcr.20139.
26. Cong F., Ning B., Ji Y. *et al. Dyes Pigm.* **2008**, *77*, 686–690. doi: 10.1016/j.dyepig.2007.07.010.
27. Medyouni R., Hallouma B., Mansour L. *et al. J. Chem. Res.* **2017**, *41*, 291–295. doi: 10.3184/174751917X14931195075571
28. Klimenko I.V., Trusova E.A., Shchegolikhin A.N., Lobanov A.V., Jurina L.V. *Fuller. Nanotub. Carb. Nanostruct.* **2022**, 30, 1, 33–39, doi: 10.1080/1536383X.2021.1976754.
29. Dąbrowski J.M., Arnaut L.G. *Photochem. Photobiol. Sci*. **2015**, *14*, 1–14. doi: 10.1039/c5pp00132c.
30. Palewska K., Sworakowski J., Lipiński J. *Opt. Mater.* **2012**, *34,* 1717–1724. doi: 10.1016/j.optmat.2012.02.009.
31. Swart G., Fourie-Müller E., Swarts J. *Molecules* **2022**, *27*, 1529. doi: 10.3390/molecules27051529.
32. Nyokong T. *Coord. Chem. Rev.* **2007**, *251*, 1707–1722. doi: 10.1016/j.ccr.2006.11.011.
33. Janczak J. *ACS Omega* **2019**, *4*, 3673−3683. doi: 10.1021/acsomega.8b03055.
34. Moon H.K., Son M., Park J.E. *et al. NPG Asia Materials* **2012**, 4, e12. doi: 10.1038/am.2012.22.
35. Carneiro Z.A., de Moraes J.C., Rodrigues F.P., *et al. J. Inorg. Biochem.* **2011**, *105*, 1035–1043. doi: 10.1016/j.jinorgbio.2011.04.011.
36. Primo F., Rodrigues M.M.A., Simioni A.R., *et al. J. Magn. Magn. Mater.* **2008**, *320*, e211–e214. doi: 10.1016/j.jmmm.2008.02.050.
37. Rak J., Pouckova P., Benes J., Vetvicka D. *Anticancer Res.* **2019**, *39*, 3323–3339. doi: 10.21873/anticanres.13475.
38. Koifman O.I., Hanack M., Syrbu S.A., Lyubimtsev A.V. *Russ. Chem. Bull., Int. Ed.* **2013**, *62*, 896–917. doi: 10.1007/s11172-013-0121-2.
39. Gradova M.A,. Ostashevskaya I.I., Gradov O.V., *et al. Macroheterocycles* **2018**, *11*, 404–411. doi: 10.6060/mhc181001g.
40. Silva E.P.O., Santos E.D., Gonçalves C.S., *et al. Laser Phys*. **2016**, *26*, 105601. doi: 10.1088/ 1054-660X/16/105601.
41. Güzel E., AtsayA., Nalbantoglu S., *et al. Dyes Pigm.* **2013**, *97*, 238–243. doi: 10.1016/j.dyepig.2012.12.027.
42. Klimenko I.V., Lobanov A.V. *Russ. J. Phys. Chem. B* **2018**, *12*, 10–16. doi: 10.1134/S1990793118010074.
43. Klimenko I.V., Lobanov A.V. *Macroheterocycles* **2020**, *13*, 142–146. doi: 10.6060/mhc200390k.
44. Klimenko I.V., Lobanov A.V., Trusova E.A. *Russ. J. Phys. Chem. B* **2019**, *13*, 964–968. doi: 10.1134/S1990793119060204.
45. Smith C.B., Days L.C., Alajroush D.R., *et al. Photochem. Photobiol.* **2022**, *98*, 17–41. doi: 10.1111/php.13467.
46. Moghassemi S., Dadashzadeh A., Narcizo de Souza P.E., *et al. Photodiagn. Photodyn Ther.* **2021**, *6*, 102555. doi: 10.1016/j.pdpdt.2021.102555.
47. Gholizadeh M., Doustvandi M.A., Mohammadnejad F. *Molecules* **2021**, *26*, 6877. doi: 10.3390/molecules26226877.
48. Kuzyniak W., Schmidt J., Glac W., *et al. Int. J. Oncol.* **2017**, *50*, 953–963. doi: 10.3892/ijo.2017.3854.
49. Huang K., Zhang H., Yan M., *et al. Dyes Pigm.* **2022**, *198*, 109997. doi: 10.1016/j.dyepig.2021.109997.
50. Velazquez F.N., Miretti M., Baumgartner M.T., *et al. Sci. Rep*. **2019**, *9*, 3010. doi: 10.1038/s41598-019-39390-0.
51. de Araújo Silva D.N., Silva N.T.D., Sena I.A.A. *Photodiagn. Photodyn. Ther*. **2020**, *31*, 101843. doi: 10.1016/j.pdpdt.2020.101843.

52. de Moraes M., Vasconcelos R.C., Figueiró J.P., *et al. Photodiagn. Photodyn. Ther*. **2015**, *12*, 592–597. doi: 10.1016/j.pdpdt.2015.10.009.
53. Gouterman M. In: *The Porphyrins. Vol. III. Physical Chemistry, Part A* (Dolphin D. Ed.), New York: Academic Press, **1978**. pp. 1–165.
54. Ogunsipe A. *FUW Trends in Science & Technology J.* **2018**, *3*(2B), 669 –681.
55. Snow A.W. Phthalocyanine Aggregation. In: *The Porphyrin Handbook*, *Vol. 17* (Kadish K.M., Smith K.M., Guilard R., Eds.), San Diego: Academic Press, **2003**. p. 129–176. doi: 10.1016/b978-0-08-092391-8.50009-1.
56. Dhami S., Phillips D. *J. Photochem. Photobiol. A* **1996**, *100*, 77–84. doi: 10.1016/S1010-6030(96)04438-3.
57. *The Porphyrin Handbook: Phthalocyanines: Properties and Materials* (Kadish K.M., Smith K.M., Guilard R., Eds.), San Diego: Academic Press, **2003**. p. 1-289.
58. Novotný M., Šebera J., Bensalah-Ledoux A., *et al. J. Mater. Res.* **2015**, *31*, 163–172. doi: 10.1557/jmr.2015.379.
59. Trusova E.A., Klimenko I.V., Afzal A.M., *et al. New J. Chem*. **2021**, *45*, 10448–10458. doi: 10.1039/d1nj01015h.
60. Berger S.D., McKenzie D.R., Martin P.J. *Philos. Mag. Lett.* **1988**, *57*, 285–290. doi: 10.1080/09500838808214715.
61. Tarakanov P.A., Simakov A.O., Pushkarev V.E., *et al. Dalton Trans.* **2023**, *52*, 2124–2134. doi: 10.1039/D2DT03371B.
62. Benesi H.A., Hildebrand J.H. *J. Am. Chem. Soc*. **1949**, *71*, 2703–2707. doi: 10.1021/ja01176a030.
63. Wang R., Yu Zh. *Acta Phys. - Chim. Sin.* **2007**, 23, 1353–1359. doi: 10.1016/S1872-1508(07)60071-0.
64. Berezin D.B., Kustov A.V., Krest'yaninov M.A., *et. al. J. Mol. Liq*. **2019**, *283*, 532–536. doi: 10.1016/j.molliq.2019.03.091.
65. Roy D., Chakraborty A., Ghosh R. *RSC Adv*. **2017**, *7*, 40563–40570. doi: 10.1039/c7ra06687b.

Received 11.04.2024
Accepted 20.05.2024